Mixed DNA/oligo(ethylene glycol) functionalized gold surfaces improve DNA hybridization in complex media

Chi-Ying Lee
National ESCA and Surface Analysis Center for Biomedical Problems, Department of Chemical Engineering, Box 351750, University of Washington, Seattle, Washington 98195-1750

Lara J. Gamble
National ESCA and Surface Analysis Center for Biomedical Problems, Department of Bioengineering, Box 351750, University of Washington, Seattle, Washington 98195-1750

David W. Grainger
Department of Chemistry, Colorado State University, Fort Collins, Colorado 80523-1872

David G. Castner[a)]
National ESCA and Surface Analysis Center for Biomedical Problems, Departments of Bioengineering and Chemical Engineering, Box 351750, University of Washington, Seattle, Washington 98195-1750

(Received 20 April 2006; accepted 7 June 2006; published 12 July 2006)

Reliable, direct "sample-to-answer" capture of nucleic acid targets from complex media would greatly improve existing capabilities of DNA microarrays and biosensors. This goal has proven elusive for many current nucleic acid detection technologies attempting to produce assay results directly from complex real-world samples, including food, tissue, and environmental materials. In this study, we have investigated mixed self-assembled thiolated single-strand DNA (ssDNA) monolayers containing a short thiolated oligo(ethylene glycol) (OEG) surface diluent on gold surfaces to improve the specific capture of DNA targets from complex media. Both surface composition and orientation of these mixed DNA monolayers were characterized with x-ray photoelectron spectroscopy (XPS) and near-edge x-ray absorption fine structure (NEXAFS). XPS results from sequentially adsorbed ssDNA/OEG monolayers on gold indicate that thiolated OEG diluent molecules first incorporate into the thiolated ssDNA monolayer and, upon longer OEG exposures, competitively displace adsorbed ssDNA molecules from the gold surface. NEXAFS polarization dependence results (followed by monitoring the N $1s \rightarrow \pi^*$ transition) indicate that adsorbed thiolated ssDNA nucleotide base-ring structures in the mixed ssDNA monolayers are oriented more parallel to the gold surface compared to DNA bases in pure ssDNA monolayers. This supports ssDNA oligomer reorientation towards a more upright position upon OEG mixed adlayer incorporation. DNA target hybridization on mixed ssDNA probe/OEG monolayers was monitored by surface plasmon resonance (SPR). Improvements in specific target capture for these ssDNA probe surfaces due to incorporation of the OEG diluent were demonstrated using two model biosensing assays, DNA target capture from complete bovine serum and from salmon genomic DNA mixtures. SPR results demonstrate that OEG incorporation into the ssDNA adlayer improves surface resistance to both nonspecific DNA and protein adsorption, facilitating detection of small DNA target sequences from these undiluted, unpurified complex biological mixtures unachievable with previously reported, analogous ssDNA/11-mercapto-1-undecanol monolayer surfaces [P. Gong, C.-Y. Lee, L. J. Gamble, D. G. Castner, and D. W. Grainger, Anal. Chem. **78**, 3326 (2006)]. © *2006 American Vacuum Society.* [DOI: 10.1116/1.2219110]

I. INTRODUCTION

Reliable, direct "sample-to-answer" capture of nucleic acid targets from complex media are sought to improve the capabilities of DNA microarrays and biosensors, particularly in field-based or remote sensing applications where sample purification of complex milieu is problematic.[1,2] This technical performance benchmark has been difficult to achieve in many nucleic acid detection technologies attempting to produce assay results directly from complex samples without amplification or pre-purification. These commonly include assays from food, tissue, and environmental materials. For example, we have recently shown that direct DNA capture from serum samples is difficult above 30% serum dilutions in buffer using surface plasmon resonance detection (SPR): DNA detection directly from 100% serum was impossible.[3,4] Such direct-from-sample detection performance requires a probe-tethered capture or detection surface that presents both functional single-strand DNA (ssDNA) probe molecules that reliably and specifically bind their DNA targets from complex solutions (e.g., signal capture), and also substrate chem-

[a)]Author to whom correspondence should be addressed; electronic mail: castner@nb.engr.washington.edu

istry that resists nonspecific adsorption (noise reduction by rejecting all other nontarget molecules such as nontarget DNA, proteins, lipids).[5] Many capture surfaces for this application have been reported, but few actually produce signal:noise ratios in complex milieu adequate for direct sample-to-answer analyses.[5] While substantial attention is directed to construction and performance evaluation of potential microarray and related biosensing surfaces for assays of simple systems (e.g., purified DNA samples in single component buffers, or pre-purified polymerase chain reaction (PCR) products), less effort has been directed to developing surfaces capable of direct detection from complex or multicomponent samples.

Numerous studies have employed thiolate-gold chemisorption to attach ssDNA oligomers to gold surfaces for biosensing experiments using SPR[6–10] and quartz crystal microbalance[11,12] techniques. The surface chemistry of gold supports can be further tailored using short alkylthiol surface diluents to control DNA-surface interactions and monolayer structure, density, hybridization efficiency and resistance toward nontarget DNA adsorption.[13–16] In previous work, we have shown that functional mixed monolayers on gold comprising both thiolated ssDNA and 11-mercapto-1-undecanol (MCU) improve DNA target capture capability over pure ssDNA monolayers.[3,4] Although MCU addition into the ssDNA adlayer improved surface hybridization efficiency by both orienting immobilized probe DNA (e.g., preventing ssDNA nonspecific interactions with the gold surface) and providing effective resistance to adsorption of noncomplementary DNA, these ssDNA/MCU surfaces were not sufficiently protein resistant to perform in complex milieu. Results of SPR-based DNA hybridization from various serum dilutions showed that both DNA hybridization kinetics and capture efficiency were adversely affected by nonspecific protein adsorption, even at a minimum serum concentration of $1v/v\%$ when compared to target capture from pure buffer. No target hybridization was detected in SPR from serum concentrations above 30%, indicating substantial interference of nonspecific protein adsorption with specific DNA capture and hybridization.

From this work and that of others,[3–5] it is clear that nonspecific protein binding represents a significant issue for performance of direct target DNA detection from biological, complex samples without pre-purification. Since sample purification or analyte enrichment (e.g., PCR) represent time- and resource-consuming processes, a key step towards improving DNA microarray and biosensor performance and selectivity in complex media is improved signal:noise ratios in direct assay; specifically, by preventing biomolecules from binding nonspecifically to assay substrates while preserving the capture efficiency of the immobilized DNA probes.

In this paper, we report improved SPR-detected DNA hybridization from complex media by incorporating oligo(ethylene glycol) (OEG) thiolated diluents into chemisorbed thiolated ssDNA monolayers, improving the prevention of nonspecific adsorption of both DNA and proteins at the SPR surface. Thiol-terminated OEG molecules replace previously used hydroxyl-terminated-alkylthiol surface diluents[3,4] because OEG units are known to be an effective chemistry to reduce nonspecific protein adsorption.[5,17–21] Mixed ssDNA/OEG monolayers are characterized by quantitatively determining surface composition, coverage and orientation of chemisorbed ssDNA using x-ray photoelectron spectroscopy (XPS) and polarization-dependent near-edge x-ray adsorption fine structure (NEXAFS). Influences of OEG diluent "backfill" on DNA target hybridization efficiency was examined using SPR with purified, unlabeled, complementary DNA in buffer. Target detection from two complex media (bovine serum and salmon genomic DNA mixtures) was then evaluated with SPR. Improved ssDNA target capture from complex sample solutions results from incorporation of protein-resistant OEG diluent components into the simple thiolated ssDNA monolayer system. These results are particularly important for improving performance and extending applications of functionalized ssDNA surfaces in biosensing assays since current requirements for sample analyte amplification (e.g., using PCR) and pre-purification to remove competing, interfering nonanalytes will remain until direct assay is possible with sufficient sensitivity and reliability.

II. EXPERIMENT

A. Materials

Silicon wafers (Silicon Valley Microelectronics, Inc., San Jose, CA) and SF-14 glass slides (Schott Glass Technology, Durea, PA) were used as substrates. High performance liquid chromatography (HPLC)-purified DNA oligomers [HS-ssDNA: 5′-HS-$(CH_2)_6$-CTGAACGGTAGCATCTTGAC-3′, complementary target: 5′-GTCAAGATGCTACCGTTCAG-3′, and noncomplementary target: 5′-CTGAACGGTAGCATCTTGAC-3′] were purchased from TriLink Biotechnologies (San Diego, CA). DNA oligomers from this vendor have been shown to contain minimal contaminants that interfere with HS-ssDNA surface assembly.[22] OEG-terminated thiols [$HS-(CH_2)_{11}-(O-CH_2-CH_2)_4-OH$] were custom synthesized at the University of Washington [>95% purity by nuclear magnetic resonance (NMR)].[23] The buffer used for both DNA probe assembly and target hybridization, denoted as STE, contained 1.0 M NaCl (Fisher, Fair Lawn, NJ), 10 mM Tris-HCl (Sigma, St. Louis, MO), and 1 mM ethylenediaminetetraacetic acid (Fisher) and was adjusted to *p*H 7.4 by adding 1.0 M NaOH. Fetal bovine serum (Premium, U.S. Origin, Hybridoma Screened, 14-901F, Lot 01103197, total protein 35–60 mg/ml) was purchased from Cambrex (Baltimore, MD), stored at −20 °C until use and diluted with STE to 1%–50% concentrations (by volume) prior to hybridization experiments. Full length salmon genomic DNA (from salmon testes, size range of 587–831 base pairs) was purchased from Sigma-Aldrich (St. Louis, MO), stored at −20 °C until use and diluted with STE to 0.1 and 1 mg/ml prior to hybridization experiments.

B. Preparation of mixed ssDNA/OEG monolayers on gold

Silicon wafers used for XPS and NEXAFS experiments were coated with 10 nm chromium and 80 nm gold (99.99%) by electron beam evaporation at pressures below 1×10^{-6} Torr. Glass slides used for SPR experiments were coated with 2 nm chromium and 50 nm gold (99.99%) under identical conditions. Mixed ssDNA/OEG monolayers of varying DNA surface coverage were fabricated using a two-step self-assembly process, analogous to that reported previously.[3,4] First, pure DNA monolayers were prepared by immersing gold-coated substrates in 1 μM HS-ssDNA solutions in STE buffer for 5 h. Samples were then rinsed thoroughly with buffer for 30 s and 18 MΩ cm water for 1 min to remove loosely bound HS-ssDNA. DNA samples were then immersed in 50 μM OEG diluent thiol solution (in degassed 18 MΩ cm water) for various timed exposures (0.5–18 h). After the specified OEG exposure time, samples were removed from solution, rinsed thoroughly in 18 MΩ cm grade water for 1 min, then blown dry with N_2 and stored under N_2 until analysis.

C. X-ray photoelectron spectroscopy

XPS analysis of DNA samples was performed on a Kratos AXIS Ultra DLD instrument equipped with a monochromatic Al $K\alpha$ x-ray source. A takeoff angle of 0° was used for all measurements. The typical x-ray spot size was 700 μm $\times 300$ μm. For each sample, an initial compositional survey scan was acquired, followed by detailed (P 2*p*, N 1*s*, O 1*s* and S 2*p*) scans using a pass energy of 80 eV. High-resolution spectra (P 2*p*, N 1*s*, O 1*s*, C 1*s*, S 2*p*, and Au 4*f*) were also acquired for the DNA samples using a pass energy of 20 eV. All binding energies were referenced to the Au 4*f* peak at 84.0 eV. Three spots on two or more replicates of each DNA sample were analyzed and averaged where atomic percent (at%) is reported. Reported compositional data were averages of values determined at each spot. Data analysis was performed with Vision Processing data reduction software (Kratos Analytical Ltd.) and CasaXPS (Casa Software Ltd.).

D. Near-edge x-ray absorption fine structure

NEXAFS spectra were performed at the National Synchrotron Light Source U7A beamline at Brookhaven National Laboratory. This beam line uses a ~85% polarized, high intensity beam, a monochromator and 600 l/mm grating which gives a full width at half maximum resolution of ~0.15 eV at the carbon *K* edge (~285 eV).[24] The monochromator energy scale was calibrated using the C $1s \rightarrow \pi^*$ transition of graphite, located at 285.35 eV. The effects of incident beam intensity fluctuations and monochromator absorption features were eliminated by normalizing all NEXAFS spectra to the signal from a pure gold (gold deposited *in situ*) control sample (I_0) and the beam flux (I_{ring}). Partial electron yield was monitored by a channeltron electron multiplier with an adjustable entrance grid bias. The bias voltage was maintained at −150 V for carbon *K*-edge spectra and −350 V for nitrogen *K*-edge spectra. Samples were mounted to allow rotation about the vertical axis to change the angle between the sample surface and the incident x-ray beam. The NEXAFS angle is defined as the angle between the incident x-ray beam and the sample surface. A near-normal incident beam is defined as the x-ray striking the surface at an angle of 70° from the sample surface while a glancing incident beam is generally 20° from the surface plane. The electric field vector (**E**) is perpendicular to the x-ray beam; therefore, when the beam is at normal incidence, the **E** vector lies parallel to the surface. A disordered system on the sample surface does not show any polarization dependence because of the random orientation of the molecules. Polarization dependence is indicative of directional alignment of the molecules in the overlayer.[25]

E. Surface plasmon resonance

The home-built SPR liquid sensing system used in this study has been described and characterized in more detail elsewhere.[26] Briefly, this SPR system is based on a planar prism (Kretschmann) configuration. The glass side of the gold-coated substrate is index matched to the prism while the functionalized surface is mechanically pressed against a milled Teflon™ flow cell. A polychromatic light beam is passed through the prism and the backside of a gold-coated substrate to excite surface plasmon waves at the metal-dielectric interface. The reflected light is analyzed with a spectrograph. During SPR measurements, STE buffer and target ssDNA solutions (1 μM complementary and non-complementary control ssDNA in STE buffer) were sequentially delivered to the SPR surface of immobilized DNA probes at a flow rate of 50 μl/min. Interactions at the gold surface were observed by monitoring the wavelength shift of the SPR reflected minimum. Data quantification was performed as reported previously[3] by first converting the measured wavelength shift into effective adlayer thicknesses (defined as the thickness that the same amount of adsorbate per unit area would have if packed at its bulk density without any trapped solvent in the adlayer), then by subsequent conversion into absolute adsorbate coverages (e.g., molecules/cm^2 of hybridized target DNA) using the method published by Jung *et al.*[26] This method requires a simple calibration of the instrument sensitivity based on SPR response to changes in bulk solution refractive index, the known index of refraction for the adsorbate and buffer, and an exponential optical sampling depth estimated from Fresnel equations. The effective adlayer thickness, *d*, was calculated using the equation

$$d = \left(\frac{\ell_d}{2}\right)\left[\frac{\Delta R}{S(\eta_a - \eta_s)}\right],$$

where ℓ_d is the decay length of the evanescent field near the gold surface (362 nm), ΔR is the measured reflected wavelength shift, *S* is the SPR system sensitivity factor (3500 reflected wavelength shift/RIU obtained by monitoring the SPR wavelength shift as a series of ethanol/water calibration

TABLE I. XPS composition data and surface coverage for pure ssDNA and mixed ssDNA/OEG monolayers on gold.[a]

Immersion time in HS-ssDNA	Immersion time in OEG	Atomic percent						Atomic ratio			Probe density (10^{13} molecules/cm^2)
		P 2*p*	N 1*s*	O 1*s*	C 1*s*	S 2*p*	Au 4*f*	P/N	O/N	C/N	
HS-ssDNA theoretical		⋯	⋯	⋯	⋯	⋯	⋯	0.3	1.7	2.8	⋯
5 h	0 h	2.0	7.7	18.1	43.1	nd[b]	29.1	0.3	2.3	5.6	4.4
5 h	0.5 h	1.2	4.5	16.7	51.1	0.9	25.7	0.3	3.7	11.4	4.1
5 h	1 h	0.9	4.0	16.7	52.4	1.3	24.7	0.2	4.2	13.2	3.6
5 h	2 h	0.7	2.5	15.4	53.2	1.3	26.9	0.3	6.1	21.1	2.1
5 h	5 h	0.4	1.6	15.0	52.3	1.5	29.2	0.3	9.6	33.7	1.2
5 h	18 h	0.3	1.0	18.7	49.9	2.0	28.1	0.3	18.5	49.5	0.7
0 h	18 h	nd	nd	13.7	52.5	1.6	32.1	⋯	⋯	⋯	0.0

[a]All standard deviations <2% with the exception of sulfur (<17%) and phosphorus (<20%).
[b]Not detectable.

solutions with varying refractive indexes of 1.333–1.3425 were injected over the gold surface following the procedure described in Ref. 26), η_a is the indices of refraction for the DNA adsorbate (1.7[27,28]), and η_s is the buffer index of refraction (1.343). Refractive indices of the calibration solutions and buffer were measured on an Abbe-3L refractometer (Bausch & Lomb, Depew, NY). Once the effective thickness of the adsorbed layer is calculated, the SPR surface coverage of adsorbed molecules can be estimated by multiplying d by the density of the pure adsorbate[26] using a density value of 1.7 g/cm^3 for hybridized dsDNA:[29]

Adsorbed DNA density (molecules/cm^2)=[effective thickness (d) (cm)]•[bulk density (N)(molecules/cm^3)].

Differences in target DNA density data measured in serum and genomic DNA dilutions by SPR were assessed using a z test and termed significant when $p \leqslant 0.05$.[30]

III. RESULTS AND DISCUSSION

A. Characterization of thiolated ssDNA/OEG monolayers by XPS and NEXAFS

1. Composition and coverage determined by XPS

Preliminary survey scans of the ssDNA/OEG monolayers indicated the presence of all elements expected from DNA (e.g., P, N, O, C, and S), OEG (O, C, and S), and substrate (Au), with no additional elements. Table I presents a summary of the surface elemental compositions and ratios for the various ssDNA/OEG monolayers as a function of OEG diluent backfill time. For the pure ssDNA monolayer surface, the experimentally obtained composition is 2 at% P, 8 at% N, 18 at% O, 43 at% C, 0 at% S, and 29 at% Au. Sulfur is not observed from the pure ssDNA monolayer due to its low stoichiometric atomic percent in a 20mer ssDNA molecule (0.2 at%), close to the XPS detection limit (~0.1 at%), and its predicted placement deep within the DNA layer at the gold surface, therefore attenuated by the DNA overlayer.[4] The P/N ratio was used to verify the stoichiometry of the DNA monolayer given that P and N are unique to DNA. The P/N ratio calculated from the atomic percents (0.3, as shown in Table I) is in good agreement with the value predicted by the stoichiometry of the DNA molecule (theoretical P/N =0.3). The O/N and C/N ratios (2.3 and 5.6) are greater than the theoretically expected values, indicating excess oxygen and carbon on the pure DNA monolayer surface likely due to the presence of adventitious hydrocarbon contamination, a presumption supported by the accuracy of the P/N atomic ratio.[4,22] After short-term OEG backfill (<1 h), increases in S and C signals correspond with decreases in P, N, O, and Au. The initial decrease in Au signal after the OEG backfill suggests that at short backfill times, the smaller OEG diluent thiols first bind into unoccupied gold sites surrounding the loosely packed DNA on the surface. With longer OEG diluent backfill time (2–18 h), the relative atomic percents of S and C continue to increase while the percent P, N, and O decrease. At these longer OEG backfill times, the Au signal increased, indicating that further OEG exposure leads to displacement of larger, more gold signal-attenuating DNA molecules from the surface by shorter OEG diluent thiols. This is consistent with previous XPS and radiolabeling studies of mixed DNA/MCU monolayers on gold where exposing DNA monolayers to a 10 μM MCU solution for increasing exposure times gradually removed ssDNA molecules from the surface.[4]

In previous studies, absolute surface densities of DNA were obtained by radiometric ^{32}P-DNA-labeling for a mixed DNA/MCU diluent thiol monolayer system and compared with at% N from XPS.[3,4] The probe-DNA surface density of the ssDNA/OEG system was calculated by correlating the XPS N 1*s* at% of ssDNA/OEG samples to that previously reported for DNA/MCU samples calibrated by radiometric measurements.[3,4] For short OEG exposure times ($\leqslant$1 h), the estimated DNA surface probe densities obtained in the present study for mixed ssDNA/OEG monolayers were similar to the DNA surface densities for the mixed DNA/MCU monolayers.[3,4] At longer OEG exposure times (>1 h), the estimated probe-DNA surface densities in mixed DNA/OEG monolayers are lower than those reported for the mixed DNA/MCU monolayers at the same backfill times. The difference in the DNA density could be explained by the slightly higher concentration of OEG diluent thiol in solution (50 μM) used in this study as compared to the 10 μM MCU solution used in the previous system.

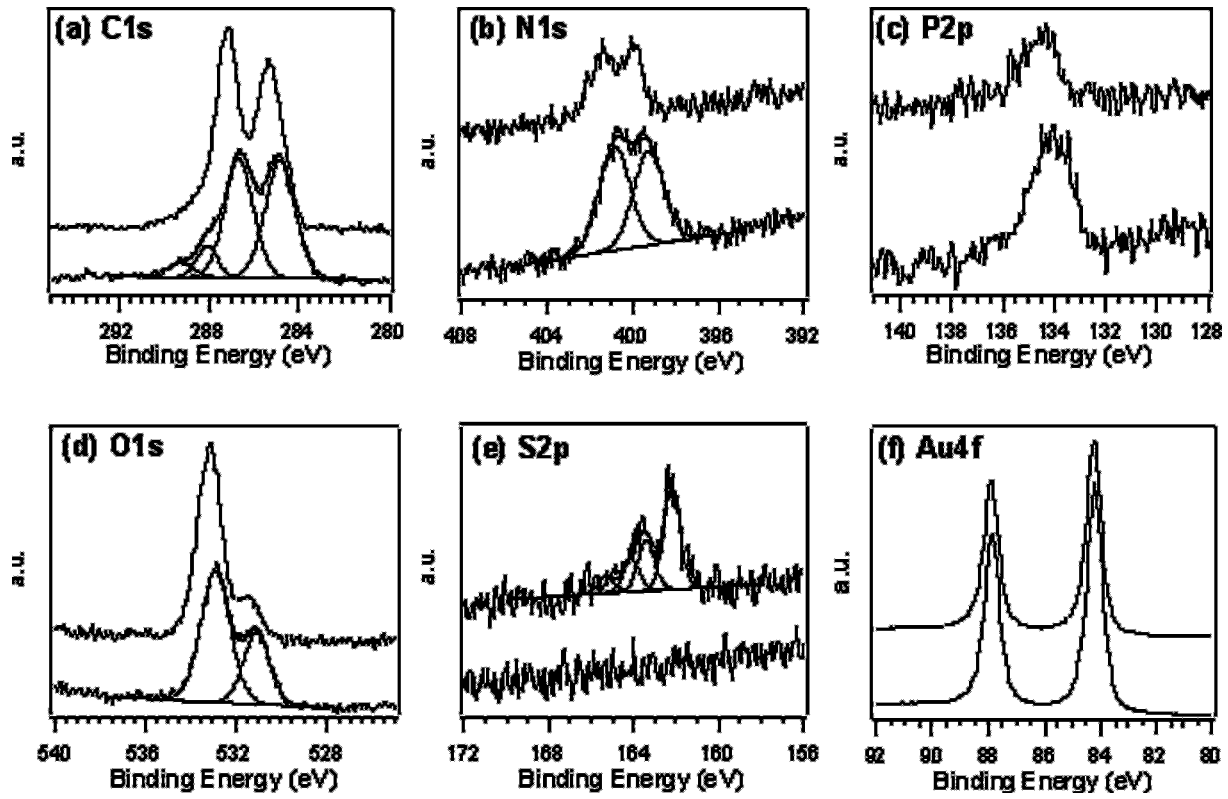

FIG. 1. High-resolution XPS (a) C 1*s*, (b) N 1*s*, (c) P 2*p*, (d) O 1*s*, (e) S 2*p* and (f) Au 4*f* spectra and fits used for area measurements from a pure ssDNA monolayer (bottom curve) and a mixed ssDNA/OEG monolayer with 1 h OEG backfill (top curve) on gold. Peak binding energies for high-resolution spectra were referenced to the Au 4*f* peak (f) at 84.0 eV. Decreases in the N 1*s* and P 2*p* peak intensities are observed after OEG backfill [(b)-(c)]. Increases in the C–O peak intensity after OEG backfill are apparent in both C 1*s* and O 1*s* spectra at 287 and 533 eV, respectively. S 2*p* peaks are observed only after OEG backfill. The binding energy (BE) of the $S_{2p3/2}$ peak [(e), 161.9 eV] is consistent with the sulfur bound to the gold surface as a thiolate species (see Ref. 33). Note that the spectra in each figure are on the same scale, offset for clarity.

High-resolution XPS spectra of the C 1*s*, S 2*p*, P 2*p*, N 1*s*, O 1*s*, and Au 4*f* regions are shown in Figs. 1(a)–1(f). Adsorption of the OEG molecules at the gold surface was also confirmed by the differences in the high-resolution C 1*s* spectra from pure ssDNA and mixed ssDNA/OEG samples [Fig. 1(a)]. The relative concentrations of the different C 1*s* carbon species are summarized in Table II as a function of OEG backfill time. The carbon species from the pure ssDNA monolayer include 48% C–C and C–H, 34% C–N and C–O, 13% N–C═O, N–C(═N)–N, N═C–N and N–C–O, and 5% urea carbon [N–C(═O)–N] with characteristic binding energies of approximately 285, 286–287, 288, and 289 eV, respectively.[4,31] Once OEG was incorporated into the DNA

TABLE II. XPS high-resolution C 1*s* chemical species of pure ssDNA and mixed ssDNA/OEG monolayers on gold.[a]

		Percentage			
Immersion time in HS-ssDNA	Immersion time in OEG	C–C, C–H (285 eV)	C–N, C–O (287 eV)	N–C(═O)–C, N–C(═N)–N, N═C–N, N–C–O (288 eV)	N–C(═O)–N (289 eV)
HS-ssDNA theoretical		20.0	45.0	27.0	8.0
5 h	0 h	48.1	34.1	12.9	4.9
5 h	0.5 h	42.7	47.2	8.2	1.9
5 h	1 h	44.8	46.0	7.3	1.9
5 h	2 h	44.4	48.1	5.9	1.6
5 h	5 h	46.1	49.8	4.1	0.0
5 h	18 h	48.6	48.8	2.6	0.0
0 h	1 h	50.2	49.8	0.0	0.0
OEG theoretical		52.6	47.4	0.0	0.0

[a]All standard deviations <2%.

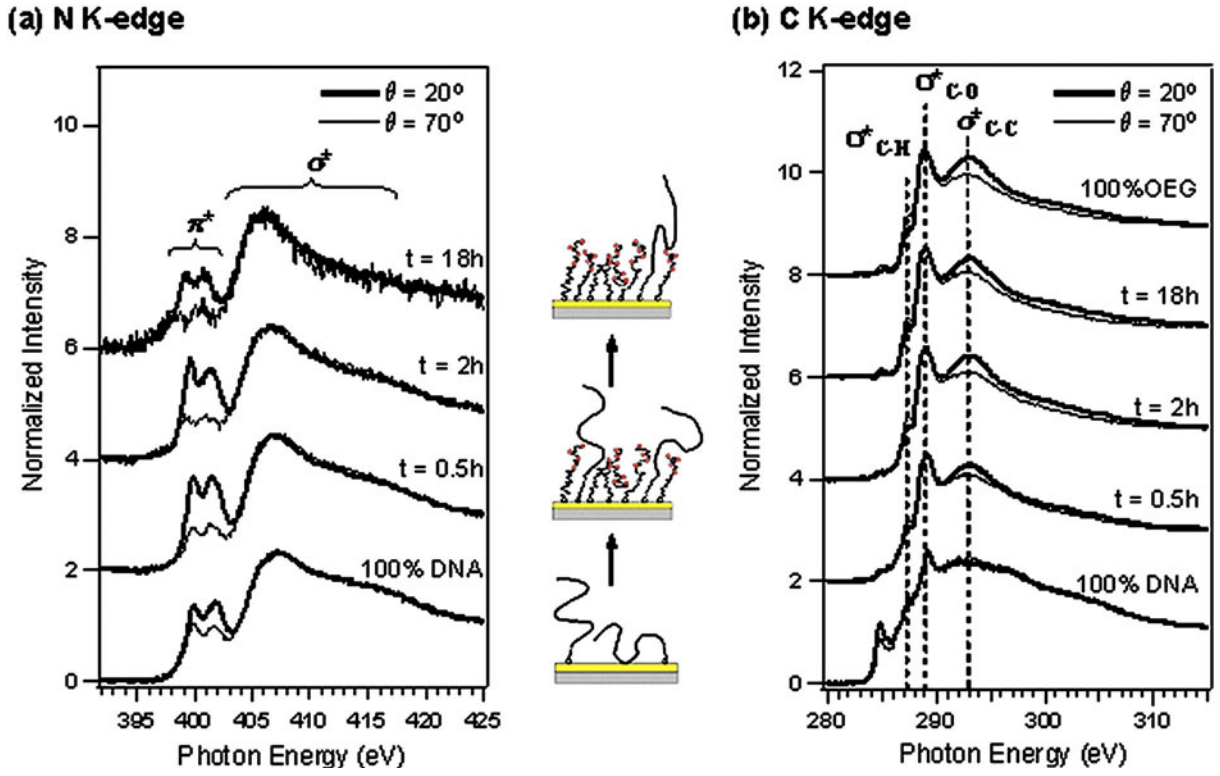

FIG. 2. Nitrogen (a) and carbon (b) *K*-edge NEXAFS spectra from pure ssDNA and mixed ssDNA/OEG monolayers on gold at near normal (70°) and glancing (20°) incident x-ray angles (t=OEG backfill time in hours). The increase in polarization dependence of nitrogen *K*-edge NEXAFS spectra with OEG backfill (a) indicates that DNA bases in the mixed monolayers are oriented more parallel to the surface than bases in the pure DNA monolayer, and that ssDNA oligomers reorient on average towards a more upright orientation on the surface upon OEG addition. The C *K*-edge spectra of the ssDNA/OEG monolayers (b) show relatively little polarization dependence. The peak at 289 eV is more pronounced in the ssDNA/OEG monolayers than the pure ssDNA monolayer because of the higher concentration of ether linkages from the OEG diluent molecules. The lack of polarization dependence for this peak suggests that the regions of the OEG molecules that contain ether linkages are disordered.

monolayer, the C–O peak intensity increased [as shown in Fig. 1(a) and Table II], and DNA carbon species intensities decreased. In addition, the O 1*s* spectra [Fig. 1(d)] show a concurrent increase in the C–O–C peak intensity (from OEG) at 533 eV, and decrease in the C═O peak intensity (from DNA) at 531 eV with the addition of OEG.[32] The N 1*s* spectra acquired for the pure DNA and mixed ssDNA/OEG samples [Fig. 1(b)] had two nitrogen peaks due to the presence of amine and aromatic nitrogen species at 399 eV and C(═O)–N, N–C(═O)–N and C(═O)–N–C(═O) species at 401 eV from the DNA molecule.[31,32] Figure 1(c) shows the P 2*p* spectra obtained from the pure DNA and mixed ssDNA/OEG monolayers. Presence of P 2*p* emission is also indicative of DNA in monolayers as it was the only source of phosphorus used during sample preparation. Decreases in the peak intensity of N 1*s* and P 2*p* peaks were observed after the addition of OEG into the DNA adlayer. Analysis of the high-resolution S 2*p* spectra [Fig. 1(e)] indicates that bound sulfur (S $2p_{3/2}$) was observed near 162 eV after the addition of OEG diluent,[33] confirming most of the OEG chains were bound to the gold substrate via thiol-gold interactions. In addition to the bound sulfur peaks at 162 eV, Fig. 1(e) shows the presence of unbound sulfur in the 164–165 eV range, possibly due to incomplete rinsing of the sample surface or retention of nonchemisorbed species.

Figures 1(a)–1(d) show that changes in XPS peak intensities, as well as shifts in the binding energies (BEs) of the C 1*s*, N 1*s*, P 2*p*, and O 1*s* regions, accompanied the addition of the OEG diluent. The C 1*s*, N 1*s*, P 2*p*, and O 1*s* XPS peaks from pure ssDNA monolayers are shifted to lower BEs than those from mixed ssDNA/OEG monolayers. (Note: Peak binding energies for all high-resolution spectra were referenced to the Au 4*f* peak at 84.0 eV as shown in Fig. 1(f)). This is in agreement with previous results,[4] where these BE shifts were found to be due to nonthiol interactions of the DNA polyanions with the gold substrate. Incorporation of OEG diluents into the ssDNA monolayer inhibited these nonspecific interactions to force DNA into a more upright position as seen with the NEXAFS results shown below.

2. DNA adlayer order and orientation measured by NEXAFS

C *K*-edge and N *K*-edge NEXAFS spectra of the mixed ssDNA/OEG monolayers were collected at near-normal (incident x-ray beam 70° to the sample surface) and glancing (20°) angles to examine the orientation and order of the ssDNA monolayers as a function OEG backfill time. NEXAFS N *K*-edge spectra for the ssDNA monolayers (0–18 h OEG backfill) are shown in Fig. 2(a). There is a π^* doublet

feature ($\Delta E = 1.7$ eV) within the 399–402 eV region of all NEXAFS N *K*-edge spectra, similar to spectra previously reported for gold-bound ssDNA[4,34,35] and dsDNA.[36] The π^* doublet feature represents an average signal over the four different nucleotide bases.[36] The lower energy π^* peak near 399–400 eV is consistent with the location of the "aromatic" nitrogen π^* peak in molecules containing nitrogen atoms in a ring structure.[37,38] The higher energy π^* peak at 401 eV is due to the nitrogen atoms in the nucleobases located next to carbonyl groups.[34,36] The broader peak above 405 eV is attributed to the N $1s \rightarrow \sigma^*$ transition.[4,34,36]

A slight polarization dependence is seen for the pure ssDNA monolayer spectra [Fig. 2(a), $t=0$] within the 399–402 eV region. The π^* doublet peak was enhanced when the x-ray beam is at glancing incidence to the sample surface ($\theta = 20°$). At glancing incidence, the electric field vector (**E**) of the polarized x-ray source is perpendicular to the surface. The overlap of this **E** vector with the antibonding π^* orbitals of the DNA bases indicates that the bases are on average nominally parallel to the gold surface. After incorporation of the OEG into the monolayer, this polarization dependence increased as the OEG molecules displace the nonthiol interactions of chemisorbed DNA polyanions with the gold substrate, thereby forcing the ssDNA molecules into a more upright position.[4,13]

Changes in the orientation of the ssDNA with increasing OEG backfill time could be monitored by comparing the dichroic ratio, ΔN_{π^*},[39,40] for the ssDNA/OEG monolayers using the formula below:

$$\Delta N_{\pi^*} = \frac{N_{\pi^*,20°} - N_{\pi^*,70°}}{N_{\pi^*,20°} + N_{\pi^*,70°}}.$$

Note that the dichroic ratios calculated here are relative and cannot be directly compared to the values from different experimental setups. Comparison of dichroic ratios derived from different experiments requires a correction factor $1/(2P-1)$, where P is the polarization degree of the synchrotron light.[39,40] The ΔN_{π^*} values for the ssDNA/OEG monolayers are shown in Fig. 3. ΔN_{π^*} increased significantly during short OEG backfill time (<1 h), reaching a maximum orientation between 0.5 and 1 h. This is similar to previous results reported for the mixed DNA/MCU monolayers where the initial increase in ssDNA orientation is proposed to arise from the removal of nonspecific interactions between the nucleobase amine groups and the gold surface[4] as shown by the BE shifts in the XPS data. Beyond 1 h of OEG backfill time ΔN_{π^*} decreased likely due to loss of ssDNA from the surface (see XPS results described above). Limited electrostatic repulsive interactions between ssDNA chains at lower ssDNA surface density would permit more disorder among the DNA chains and facilitate some nucleotide-surface reengagement as shown by the data.

The C *K*-edge spectra of the ssDNA/OEG monolayers [Fig. 2(b)] show relatively little polarization dependence. The peak at 293 eV has been assigned to the C–C species (σ^*_{C-C}).[41,42] With the incorporation of OEG diluent thiols, this peak was slightly enhanced when the x-ray beam was at glancing (20°) incidence to the sample surface, indicating that the C–C bonds in the OEG molecules were oriented nominally perpendicular to the surface. The peak at 287.4 eV is attributed to the transition from the C $1s$ to the C–H* orbital.[41,42] With the addition of OEG, this peak was slightly enhanced when the x-ray beam was at normal (70°) incidence to the sample surface, indicating the C–H σ^* bonds are on average parallel to the surface. The polarization dependence of the σ^*_{C-C} and σ^*_{C-H} peaks was similar to the spectra previously reported for hydrocarbon adlayers[41] and Langmuir–Blodgett films.[42] The peak at 289 eV, attributed to the transition from the C $1s$ to C–O* orbital, is more pronounced in the ssDNA/OEG monolayers than the pure ssDNA monolayer because of the higher concentration of ether linkages from the OEG diluent molecules. The lack of any appreciable polarization dependence for the C–O ether peak suggests that the terminal ethylene glycol regions of the OEG molecules are disordered.

B. SPR measurement of DNA hybridization on ssDNA/OEG monolayers

1. Hybridization in purified DNA target solutions

Previous work has shown that DNA surface hybridization is dependent on MCU diluent backfill time since the introduction of MCU affects both immobilized-ssDNA density and orientation.[3,4] Here, SPR measurements were made to investigate DNA hybridization efficiency as a function of OEG diluent backfill time (0.5–18 h) with purified, unlabeled DNA targets (1 μM) in STE buffer [see Fig. 4(a)]. To test the specificity of the ssDNA/OEG monolayers, a noncomplementary ssDNA strand (1 μM) was used as a control [Fig. 4(a), step 1]. No detectable hybridization signal was obtained from the noncomplementary experiments after rinsing the probe surfaces with buffer (Fig. 4(a), step 2). This suggests that the OEG diluent effectively prevents noncomplementary short ssDNA sequences from binding nonspecifically to the surface. With the injection of 1 μM

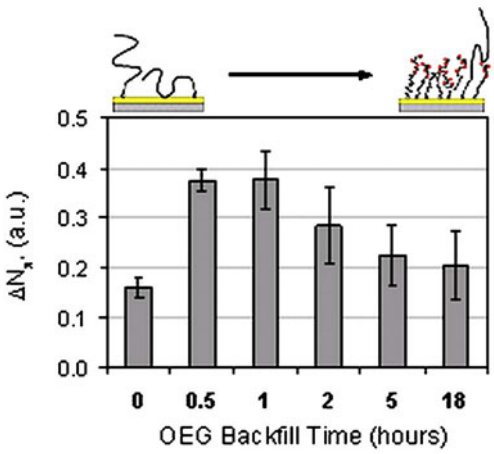

FIG. 3. Dichroic ratio (ΔN_{π^*}) for pure ssDNA and mixed ssDNA/OEG monolayers on gold as a function of OEG backfill time. ΔN_{π^*} reaches its maximum at ~0.5–1 h of OEG exposure, after which ΔN_{π^*} decreases due to the loss of ssDNA from surface.

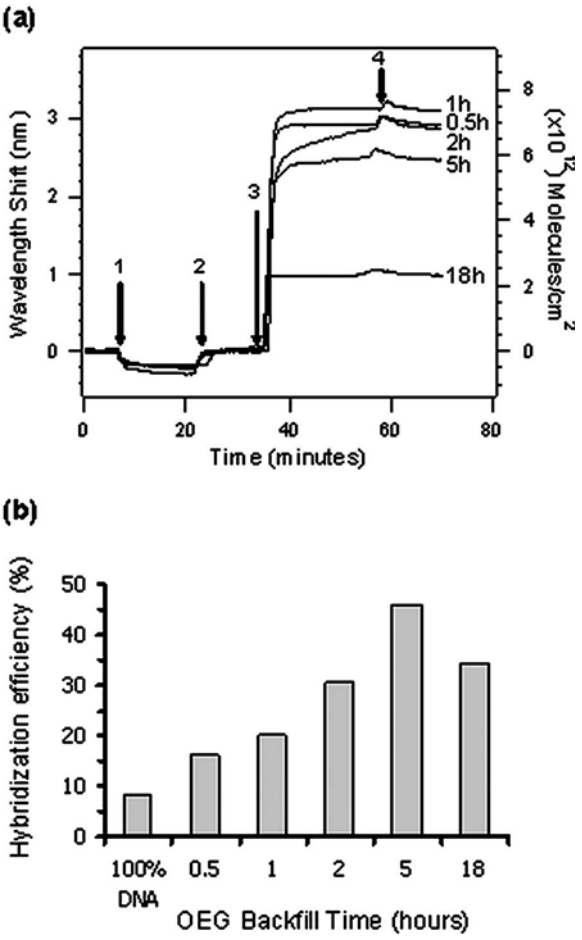

FIG. 4. Real-time SPR measurement of target DNA hybridization on ssDNA/OEG probe surfaces from STE buffer demonstrating the effects of OEG diluent backfill on DNA target hybridization (a). After establishing a measurement base line by introducing buffer to the probe surface, noncomplementary DNA (1 μM) in running buffer was injected to test nonspecific target binding onto the probe surface (1). As the noncomplementary DNA adsorption reaches saturation, the noncomplementary DNA solution was replaced with pure running buffer to reestablish the base line (2). Complementary DNA target (1 μM) was then injected to determine amounts of hybridization (3). As DNA hybridization approached saturation, the complementary DNA solution was replaced with pure running buffer to rinse away loosely bound DNA molecules from the probe surface (4). Data indicate that target hybridization reaches a maximum at 1 h OEG backfill (surface density of 3.6×10^{13} probe molecules/cm^2). The estimated hybridization efficiency for each ssDNA/OEG probe surface as a function of OEG backfill time (b).

complementary ssDNA targets (Fig. 4(a), step 3), significant complementary strand hybridization was detected on the ssDNA/OEG probe surfaces, even after buffer rinse (Fig. 4(a), step 4). Amounts of complementary DNA hybridized onto these mixed ssDNA/OEG probe surfaces range from 2.4 to 7.2×10^{12} molecules/cm^2, depending on the ssDNA probe densities.[2,13] These values are comparable to amounts of DNA target hybridized by a ssDNA/MCU system reported previously.[3] As seen in Fig. 4(a), target DNA hybridization signal reaches a maximum on probe surfaces with 1 h OEG diluent backfill (a surface ssDNA probe density of 3.6×10^{13} molecules/cm^2), after which target hybridization decreases due to significant displacement of DNA probes off the monolayer surface by OEG, as determined by XPS measurements. Target hybridization efficiency (defined as target density divided by probe density and multiplied by 100) on the ssDNA/OEG probe surfaces can be estimated from the probe densities (Table I) and target densities [Fig. 4(a)]. The estimated target hybridization efficiency values are presented in Fig. 4(b) as a function of OEG backfill time. Pure ssDNA probe surfaces show 8% hybridization efficiency, increasing to a maximum of 46% at intermediate probe density then decreasing at lower probe density.

2. Hybridization in bovine serum and salmon genomic DNA mixtures

The capability to capture target DNA via hybridization directly from complex mixtures (e.g., PCR mix, serum, tissue lysates, food and environmental samples) without extensive amplification or purification is desirable for improved microarray and biosensing assays. SPR was used to investigate the selectivity of the ssDNA/OEG probe surface from two biological media, bovine serum and salmon genomic DNA. Serum contains high concentrations of over 200 different proteins[43] (total protein 35–60 mg/ml) while genomic DNA mixtures contain large molecular weight DNA fragments (in a size range of 600–900 base pairs) where the vast amount of nucleic acid sequences do not correspond to the target sequence. Both conditions present significant non specific background species more relevant to real world assay goals than buffer-based capture. These SPR experiments were performed using DNA-probe surfaces with 1 h OEG backfill time since this condition provides maximum amount of target capture (see Fig. 4 SPR results above) from purified DNA targets.

For hybridization experiments from serum, the concentration of the target sequence was kept at 1 μM while the serum concentration was varied from 1 to 100 vol % (i.e., the target sequence is mixed with different serum dilutions up to full strength native serum). To determine the amount of specific target capture from various serum dilutions, the SPR response from negative controls consisting of noncomplementary DNA sequences in the same serum concentrations was also monitored. Figure 5 shows the SPR response of the interactions of ssDNA/OEG probe surfaces with both complementary (Fig. 5, curve 1) and noncomplementary (Fig. 5, curve 2) DNA sequences in 1 vol % [Fig. 5(a)] and 100 vol % [Fig. 5(b)] serum. Note that the SPR response for 100% serum solutions is beyond the range of plotted wavelength values due to a significant increase in the bulk solution refractive index. To determine the amount of specific DNA hybridization, the response from noncomplementary DNA in *n*% serum was subtracted from complementary DNA in *n*% serum as illustrated by the dashed curve in Fig. 5. As seen in Fig. 5, the amount of specific target hybridization, or binding, decreased significantly as serum concentration was increased from 1% to 100%. This is consistent with previous reports on identical DNA target hybridization using the mixed DNA/MCU probe adlayer SPR assay.[3] Comparison of Fig. 5(a) with Fig. 5(b) suggests that this loss of

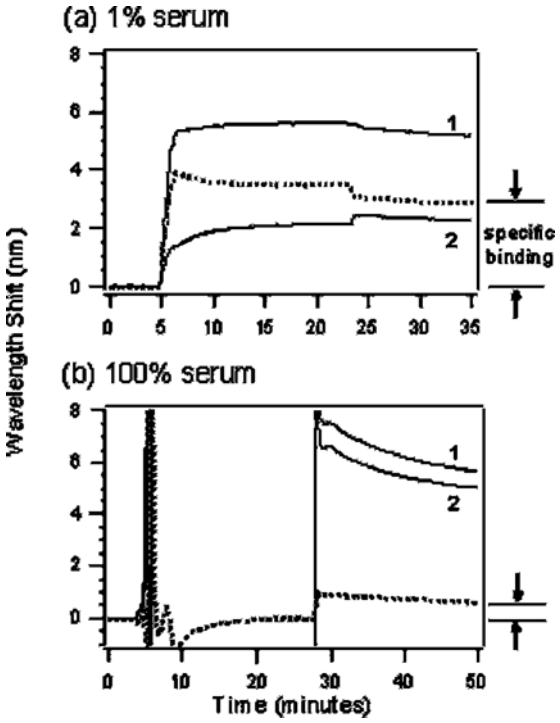

FIG. 5. SPR hybridization results for target capture performed in solutions containing (a) 1% and (b) 100% serum. The curves show responses from the SPR when probe surfaces were exposed to complementary (curve 1) and noncomplementary (curve 2) DNA in *n*% serum at approximately 5 min and rinsed with buffer when adsorption saturation was reached at approximately 25 min. DNA hybridization is obtained by subtracting the SPR response for the noncomplementary DNA in *n*% serum from the SPR response for the complementary DNA in *n*% serum solution (dashed line). Note that the SPR response to 100% serum is out of range of the plotted wavelength values due to significant increase in the bulk solution refractive index.

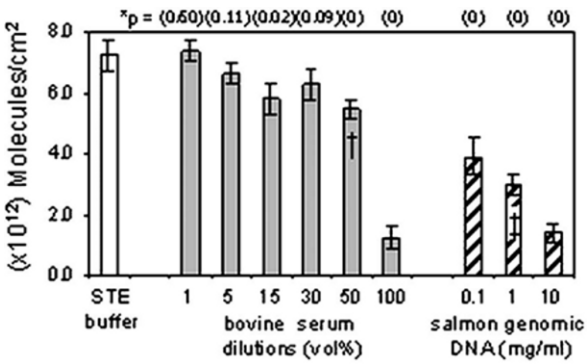

FIG. 6. Amounts of DNA target hybridization from buffer (white), bovine serum (gray), and salmon genomic DNA (stripes) dilutions as determined by SPR using the procedure described by Fig. 5. Hybridized target molecular densities were estimated using the wavelength shift due to DNA hybridization. ($^*P$ indicates p value when compared with hybridized target density in STE buffer. † indicates $p=0$ when the 50 vol % serum hybridization results are compared to those from 5, 15, and 30 vol % serum. ‡ indicates $p<0.03$ when the 1 mg/ml salmon genomic DNA hybridization results are compared to the 0.1 mg/ml salmon genomic DNA hybridization results.)

specific target capture is due to increased nonspecific serum protein adsorption onto the probe surface with increasing serum concentration. This increased serum protein adsorption is supported by the higher SPR wavelength shift from noncomplementary DNA in 100% serum (5 nm) compared to noncomplementary DNA in 1% serum (2.5 nm). DNA target hybridization at a constant concentration of 1 μM from various serum concentrations is summarized from SPR signals as molecular densities in Fig. 6. These bound molecular densities were estimated using the SPR wavelength shift calculated from that due to specific DNA hybridization using equations and assumptions described in the Sec. II. As seen in Fig. 6, target hybridization on ssDNA/OEG surfaces decreases only slightly (by roughly 20%) as the serum concentration is increased to 50%. In undiluted serum (100%), target hybridization on the probe surface was reduced by approximately 80%, but still well above base line noise, to 1.3×10^{12} molecules/cm^2. Comparing these results to data previously reported for DNA hybridization on ssDNA/MCU probe surfaces where target capture via hybridization is reduced by 50% in 15% serum and essentially zero beyond 50% serum,[3] OEG backfill significantly improves the selectivity of the DNA-probe surface, allowing target detection directly from undiluted serum. One conclusion is that an OEG background is more effective at preventing nonspecific protein binding than the hydroxyl-terminated MCU alkylthiol diluted surfaces, making it possible to detect a given target DNA strand within a solution containing substantial protein background.

The performance of the ssDNA/OEG probe surface was further evaluated using fragmented salmon genomic DNA mixtures where the vast majority of nucleic acid sequences do not correspond to the target sequence. The probe surface was exposed to 1 μM (approximately 6×10^{-3} mg/ml) complementary target solutions containing varying concentrations (0.1, 1.0, and 10 mg/ml) of genomic DNA. The target to genomic DNA ratio (wt/wt) is approximately 1:16, 1:160, and 1:1600 for 0.1, 1.0, and 10 mg/ml of genomic DNA mixtures, respectively. Samples containing only the genomic DNA mixture (at 0.1, 1.0, and 10 mg/ml) were used as negative controls to monitor the amount of nonspecific DNA adsorption onto the probe surface. Figure 7 shows the SPR response obtained when the ssDNA/OEG surface was exposed to complementary (Fig. 7, curve 1) DNA target sequences (1 μM) in 0.1 [Fig. 7(a)] and 10 mg/ml [Fig. 7(b)] genomic DNA, and the corresponding negative controls (Fig. 7, curve 2). Comparison of curve 2 in Figs. 7(a) and 7(b) indicate that the amount of nonspecific DNA adsorption onto the probe surface increases with increasing genomic DNA concentration. The amount of specific DNA hybridization is determined by subtracting the SPR response to the negative control from the SPR response to solutions containing complementary DNA in *n* mg/ml of genomic DNA as illustrated by the dashed curves in Fig. 7. Captured molecular densities of DNA target hybridization from various genomic DNA concentrations in Fig. 7 were again estimated using the wavelength shift due to DNA hybridization (see Sec. II) and are summarized, together with serum capture data from Fig. 5, in Fig. 6. The data demonstrate that while the ssDNA/OEG functionalized gold surface is not completely

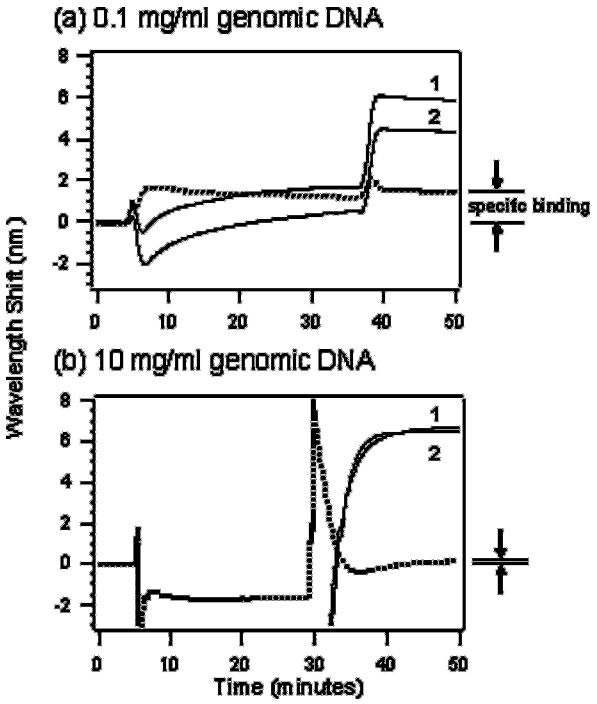

FIG. 7. SPR hybridization results for target capture performed in solutions containing (a) 0.1 and (b) 10 mg/ml of salmon genomic DNA. The curves show responses from the SPR when probe surfaces were exposed to complementary DNA in *n* mg/ml genomic DNA (curve 1) and *n* mg/ml genomic DNA without target DNA sequence at approximately 5 min. The surface was rinsed with buffer when adsorption saturation was reached at approximately 35 min. DNA hybridization is obtained by subtracting curve 2 from curve 1 (dashed line). Note that the SPR response to 10 mg/ml genomic DNA mixture is out of range of the plotted wavelength values due to significant increase in the bulk solution refractive index.

nonfouling for complex DNA mixtures, detection of the DNA target sequence from these solutions is still possible and well above base line noise, but compromised compared to dilute serum or pure buffer.

Given that a single mammalian cell contains up to 100 pg of DNA, and that only one specific sequence from this collective amount is sought in a given capture assay, very few, if any, detection methods conveniently and reliably isolate and detect this target, even when purified from gram masses of cells. PCR is, therefore, ubiquitously exploited to generate sufficient (i.e., $\sim 10^{15}$/ml), short copies of the target sequence to detect in different assay formats. Typical DNA detection limits for many microarray formats are 10–100 femtomolar DNA target from buffer solutions (i.e., 10^{-14} moles DNA/l $= 10^{9}$ DNA target molecules/l $= 10^{3}$ DNA target molecules/μl). These detection limits in most fluorescence-based microarray assays correspond to surface-captured densities of $\sim 10^{12}$–10^{13} target molecules/cm^2. Detection limits from most assays in serum are several orders of magnitude poorer.[44] This study addresses the challenge of detecting DNA hybridization from complex media by using DNA/OEG surface chemistry that improves resistance to the nonspecific adsorption of proteins, noncomplementary DNA, etc., that otherwise would prevent the DNA hybridization.

IV. CONCLUSIONS

This study investigates a more relevant assay procedure and model DNA biosensing surface for diagnostics applications compared to simple buffer detection. Increasingly, nucleic acid assay is desired directly from PCR mixtures (i.e., from *q*-PCR or on chip), or from tissue, cell, food, or biological samples without pre-purification steps that cost both time and labor, and that limit field or remote deployment. Few existing assays can demonstrate such performance in direct "sample-to-answer" formats, and even fewer DNA capture reports test such conditions. Most DNA detection by surface capture (the most common nucleic acid assay format) reports assay from DNA in buffers, often claiming detection performance that is actually of limited practical relevance. This study demonstrates the use of protein-resistant OEG diluent molecules in SPR surfaces to improve DNA target capture from complex biological mixtures including bovine serum and salmon genomic DNA. The composition, orientation, and target hybridization efficiency of sequentially self-assembled ssDNA/OEG monolayers on gold were characterized in detail using the high-resolution surface analytical methods, XPS, NEXAFS, and SPR. Surface composition of various ssDNA/OEG monolayers was determined using XPS. XPS nitrogen atomic percent was used to calculate surface coverage of the ssDNA in the mixed monolayer system, as calibrated by previous radio-labeling results.[3] Surface coverage of the ssDNA in the mixed ssDNA/OEG monolayer decreased steadily with increasing OEG diluent backfill time. XPS and angle-resolved NEXAFS measurements showed that pure ssDNA did not assemble into ordered monolayers, possibly due to nonspecific interactions of the DNA bases with the gold surface. Incorporation of the OEG diluent thiol into the ssDNA adlayer initially improved the immobilized ssDNA orientation and order by displacing these nonspecific DNA-gold interactions, as demonstrated by XPS peak shifts and NEXAFS results showing an increase in the dichroic ratio (ΔN_{π^*}) with maximum orientation at 0.5–1 h backfill time. Target hybridization on the various ssDNA/OEG monolayers with purified DNA targets in buffer indicated that DNA surface hybridization is influenced by immobilized-ssDNA density and orientation. Maximum target DNA hybridization was observed on probe surfaces with 1 h of OEG diluent backfill (a surface ssDNA probe density of 3.6×10^{13} molecules/cm^2), after which target hybridization decreased due to significant OEG displacement of DNA probes off the monolayer surface. SPR measurements of target DNA hybridization from bovine serum and salmon genomic DNA mixtures demonstrated that OEG incorporation into the ssDNA adlayer improved surface resistance to both nonspecific protein and DNA adsorption, allowing detection of small DNA target sequences from concentrated, complex biological mixtures. While exhibiting significantly improved signal:noise ratios comparted to previous assays, observed SPR DNA target detection signal in 100% undiluted nonspecific serum or full-length genomic DNA competition is significantly reduced compared to that from DNA target in buffer. These differ-

ences between assay results from buffer versus those in complex media demonstrate the challenge for nucleic acid capture in the presence of substantial competing nonspecific adsorption noise. Microarray or surface capture nucleic acid assays will need to achieve improved signal:noise ratios from such media in order to perform adequately in field-based or direct sample-to-answer analyses.

ACKNOWLEDGMENTS

The authors gratefully acknowledge support from NESAC/Bio (NIH Grant No. EB-002027) and NIH Grant No. EB-001473. NEXAFS studies were performed at the NSLS, Brookhaven National Laboratory, which is supported by the U.S. Department of Energy, Division of Materials Science and Division of Chemical Sciences. D. Fischer, C. Campbell, P. Gong and J. Apte are thanked for their discussions and assistance with the experiments involved in this study.

[1]S. Hahn, S. Mergenthaler, B. Zimmermann, and W. Holzgreve, Bioelectrochemistry **67**, 151 (2005).
[2]P. A. E. Piunno and U. J. Krull, Anal. Bioanal. Chem. **381**, 1004 (2005).
[3]P. Gong, C.-Y. Lee, L. J. Gamble, D. G. Castner, and D. W. Grainger, Anal. Chem. **78**, 3326 (2006).
[4]C.-Y. Lee, P. Gong, G. M. Harbers, D. W. Grainger, D. G. Castner, and L. J. Gamble, Anal. Chem. **78**, 3316 (2006).
[5]M. Lochhead, C. A. Greef, P. Gong, and D. W. Grainger, in *Microarrays: Methods and Protocols (Methods in Molecular Biology)*, 2nd ed. (Humana Press, Totowa, NJ, in press).
[6]R. Georgiadis, K. P. Peterlinz, and A. W. Peterson, J. Am. Chem. Soc. **122**, 3166 (2000).
[7]A. W. Peterson, R. J. Heaton, and R. Georgiadis, J. Am. Chem. Soc. **122**, 7837 (2000).
[8]A. W. Peterson, R. J. Heaton, and R. M. Georgiadis, Nucleic Acids Res. **29**, 5163 (2001).
[9]A. W. Peterson, L. K. Wolf, and R. M. Georgiadis, J. Am. Chem. Soc. **124**, 14601 (2002).
[10]B. P. Nelson, T. E. Grimsrud, M. R. Liles, R. M. Goodman, and R. M. Corn, Anal. Chem. **73**, 1 (2001).
[11]Y. K. Cho, S. Kim, Y. A. Kim, H. K. Lim, K. Lee, D. S. Yoon, G. Lim, Y. E. Pak, T. H. Ha, and K. Kim, J. Colloid Interface Sci. **278**, 44 (2004).
[12]F. Caruso, E. Rodda, D. N. Furlong, and V. Haring, Sens. Actuators B **41**, 189 (1997).
[13]R. Levicky, T. M. Herne, M. J. Tarlov, and S. K. Satija, J. Am. Chem. Soc. **120**, 9787 (1998).
[14]T. M. Herne and M. J. Tarlov, J. Am. Chem. Soc. **119**, 8916 (1997).
[15]H. J. Lee, Y. Li, A. W. Wark, and R. M. Corn, Anal. Chem. **77**, 5096 (2005).
[16]T. T. Goodrich, H. J. Lee, and R. M. Corn, J. Am. Chem. Soc. **126**, 4086 (2004).
[17]L. K. Ista, H. Y. Fan, O. Baca, and G. P. Lopez, FEMS Microbiol. Lett. **142**, 59 (1996).
[18]K. L. Prime and G. M. Whitesides, J. Am. Chem. Soc. **115**, 10714 (1993).
[19]K. Bergstrom, K. Holmberg, A. Safranj, A. S. Hoffman, M. J. Edgell, A. Kozlowski, B. A. Hovanes, and J. M. Harris, J. Biomed. Mater. Res. **26**, 779 (1992).
[20]C. Palegrosdemange, E. S. Simon, K. L. Prime, and G. M. Whitesides, J. Am. Chem. Soc. **113**, 12 (1991).
[21]C. Boozer, J. Ladd, S. F. Chen, Q. Yu, J. Homola, and S. Y. Jiang, Anal. Chem. **76**, 6967 (2004).
[22]C. Y. Lee, H. E. Canavan, L. J. Gamble, and D. G. Castner, Langmuir **21**, 5134 (2005).
[23]K. E. Nelson, L. Gamble, L. S. Jung, M. S. Boeckl, E. Naeemi, S. L. Golledge, T. Sasaki, D. G. Castner, C. T. Campbell, and P. S. Stayton, Langmuir **17**, 2807 (2001).
[24]J. L. Lenhart, R. L. Jones, E. K. Lin, C. L. Soles, W. L. Wu, D. A. Fischer, S. Sambasivan, D. L. Goldfarb, and M. Angelopoulos, J. Vac. Sci. Technol. B **20**, 2920 (2002).
[25]J. Stohr, *NEXAFS Spectroscopy* (Springer, New York, 1992).
[26]L. S. Jung, C. T. Campbell, T. M. Chinowsky, M. N. Mar, and S. S. Yee, Langmuir **14**, 5636 (1998).
[27]P. G. Wu, B. S. Fujimoto, L. Song, and J. M. Schurr, Biophys. Chem. **41**, 217 (1991).
[28]R. E. Harrington, J. Am. Chem. Soc. **92**, 6957 (1970).
[29]J. E. Darnell and H. Lodish, *Molecular Cell Biology* (Scientific American, New York, 1990).
[30]J. Mandel, *The Statistical Analysis of Experimental Data* (Dover, New York, 1984).
[31]C. J. May, H. E. Canavan, and D. G. Castner, Anal. Chem. **76**, 1114 (2004).
[32]G. Beamson and D. Briggs, *High Resolution XPS of Organic Polymers* (Wiley, West Sussex, 1992).
[33]D. G. Castner, K. Hinds, and D. W. Grainger, Langmuir **12**, 5083 (1996).
[34]N. T. Samuel, C.-Y. L. Lee, L. J. Gamble, D. A. Fisher, and D. G. Castner, J. Electron Spectrosc. Relat. Phenom. **152**, 134 (2006).
[35]D. Y. Petrovykh, V. Perez-Dieste, A. Opdahl, H. Kimura-Suda, J. M. Sullivan, M. J. Tarlov, F. J. Himpsel, and L. J. Whitman, J. Am. Chem. Soc. **128**, 2 (2006).
[36]J. N. Crain, A. Kirakosian, J. L. Lin, Y. D. Gu, R. R. Shah, N. L. Abbott, and F. J. Himpsel, J. Appl. Phys. **90**, 3291 (2001).
[37]A. G. Shard, J. D. Whittle, A. J. Beck, P. N. Brookes, N. A. Bullett, R. A. Talib, A. Mistry, D. Barton, and S. L. McArthur, J. Phys. Chem. B **108**, 12472 (2004).
[38]M. Zwahlen, D. Brovelli, W. Caseri, and G. Hahner, J. Colloid Interface Sci. **256**, 262 (2002).
[39]M. Zharnikov, Y. Ouchi, M. Hasegawa, and A. Scholl, J. Phys. Chem. B **108**, 859 (2004).
[40]M. G. Samant, J. Stohr, H. R. Brown, T. P. Russell, J. M. Sands, and S. K. Kumar, Macromolecules **29**, 8334 (1996).
[41]G. Hahner, M. Kinzler, C. Thummler, C. Woll, and M. Grunze, J. Vac. Sci. Technol. A **10**, 2758 (1992).
[42]D. A. Outka, J. Stohr, J. P. Rabe, and J. D. Swalen, J. Chem. Phys. **88**, 4076 (1988).
[43]N. L. Anderson and N. G. Anderson, Mol. Cell Proteomics **1**, 845 (2002).
[44]N. L. Rosi and C. A. Mirkin, Chem. Rev. (Washington, D.C.) **105**, 1547 (2005).